The effect of compressibility on grid-point and time-step requirements for simulations of wall-bounded turbulent flows

By K. P. Griffin, L. Fu† AND P. Moin

1. Motivation and objectives

In high-Reynolds-number flows, the computational cost of a direct numerical simulation (DNS) is often intractably large. For this reason, it is essential to be able to predict its cost in advance. Furthermore, cost estimates also inform if physical models (sub-grid-scale models, wall models, etc.) can be deployed to reduce the cost of a simulation to a tractable size. Accurate estimates can also guide the construction of tailored spatial meshes, and these estimates can inform decisions regarding code development, such as to support hierarchical meshes or to treat temporal integration of viscous or all terms implicitly.

In this work, we aim to develop estimates for the grid-point and time-step requirements for DNS of compressible flows. Although several works have quantified the cost of simulations of incompressible turbulent flows (Chapman 1979; Choi & Moin 2012; Yang & Griffin 2021), they did not consider how compressibility leads to mean property variations (e.g. density and viscosity), which alters the size of turbulence structures and thus the required grid-point and time-step requirements for simulations. In addition, in a cold-wall compressible boundary layer, a sharp peak in the temperature profile can form, and the cost of resolving it is also considered. Also considered is the more stringent time-step requirement due to mean property variations.

The remainder of this paper is organized as follows. In Section 2, a method is presented, which estimates the wall-normal variation of mean properties of the flow. In Section 3, the results for grid-point requirements for compressible flows are presented. In Section 4, the results for time-step requirements for compressible flows are presented. Concluding remarks are given in Section 5.

2. Mean profiles for the wall-normal variation of flow properties

In a compressible flow, the mean fluid properties can vary significantly in the wall-normal direction. Because the property values will affect resolution requirements in space and time, this section estimates the mean property profiles by combining several existing models for canonical flows and discusses the applicability of these estimates to more complex flows.

We begin with the thin boundary layer assumption, which implies that the pressure is invariant with wall-normal distance, i.e., $P[y] \approx P[y = 0]$, which is denoted as the wall pressure P_w. Consequently, it is approximately equal to the boundary-layer-edge pressure

† Currently at Hong Kong University of Science and Technology

P_e. We consider the case of an ideal gas obeying Sutherland's viscosity law, which implies

$$\rho[y] = \frac{1}{T[y]}\frac{P_w}{R}, \tag{2.1}$$

$$\mu[y] = \mu_{ref}\left(\frac{T[y]}{T_{ref}}\right)^{3/2}\frac{T_{ref}+S}{T[y]+S}, \tag{2.2}$$

where T is the temperature, ρ is the density, R is the gas constant, μ is the dynamic viscosity, T_{ref} and μ_{ref} are viscosity reference data, and S is the Sutherland temperature.

In order to close these estimates for the mean property profiles $\rho[y]$ and $\mu[y]$, we must estimate the temperature $T[y]$, but this is coupled to the velocity profile $U[y]$. The velocity profile can be described with an incompressible velocity law of the wall and a compressible velocity transformation that accounts for compressibility effects. The former is given by

$$U^+_{incomp} = \begin{cases} y^+ + a_1(y^+)^2 & y^+ \le y_s \\ \frac{1}{\kappa}\ln(y^+) + B & y^+ \ge y_s, \end{cases} \tag{2.3}$$

where $\kappa = 0.41$ is the von Kármán constant and $B = 5.2$ is the log intercept. Requiring that the velocity profile have continuous value and derivative implies that $a_1 = -0.0192$ and $y_s = 23.3$. This model does not account for the boundary layer wake. We explored including the wake model of Griffin *et al.* (2021*a*) but found that it has little effect on the grid-point estimates because the small scales in the wake region contain the largest turbulence scales, so they make a relatively small contribution to the grid-point estimates and will not contribute to the time-step restriction.

To apply this profile to a compressible flow, we deploy the total-stress-based compressible velocity transformation of Griffin *et al.* (2021*b*) because unlike existing transformations, it is suitable for channels and boundary layers with and without heat transfer. The transformation uses the viscous scaling arguments of Trettel & Larsson (2016) and Patel *et al.* (2016) in the near-wall viscous region and uses a modified version of the turbulence equilibrium arguments of Zhang *et al.* (2012) for the log region. The transformation is given by

$$U^+_{incomp} = \int S^+_t dy^*, \tag{2.4}$$

where U^+_{incomp} is the transformed velocity (which is assumed to be Mach invariant and thus equal to the incompressible law of the wall), $y^* = y\sqrt{\tau_w \rho}/\mu$ is the semi-local non-dimensionalization of the wall-normal coordinate (Huang *et al.* 1995; Coleman *et al.* 1995), and S^+_t is a non-dimensionalization of the mean shear, which is defined as

$$S^+_t = \frac{S^+_{eq}}{1 + S^+_{eq} - S^+_{TL}}. \tag{2.5}$$

Here $S^+_{eq} = 1/\mu^+ dU^+/dy^*$, $S^+_{TL} = \mu^+ dU^+/dy^+$, and U is the untransformed compressible velocity profile.

Lastly, an estimate for the temperature profile is obtained. Although temperature laws of the wall exist, they are generally less universal than the velocity law of the wall in flows with significant property variations (Guo *et al.* 2019). For the present work, we instead deploy an algebraic relationship between the temperature profile and the velocity profile. One such relation was proposed by Crocco (1932) and Busemann (1931) by observing the analogy between the conservation equations for momentum and energy

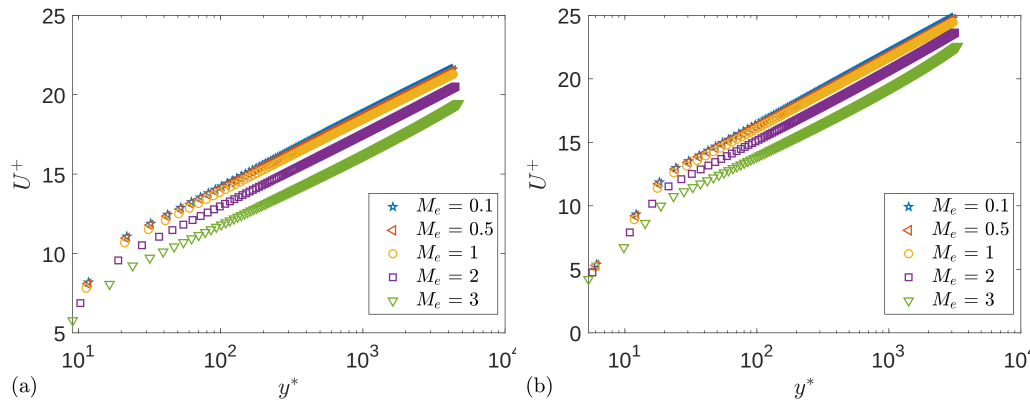

FIGURE 1. Velocity profiles for boundary layers with $M_e = \{0.1, 0.5, 1.0, 2.0, 3.0\}$ and $Re_{\delta,e} = 7.5e4$. (a) $T_e/T_w = 3/2$. (b) $T_e/T_w = 1$.

under the assumption of unity Prandtl number. Walz (1969) derived an improved relation to account for a non-unity Prandtl number. Duan & Martín (2011) introduced an empirical improvement to this relation for cold-wall boundary layers. Zhang *et al.* (2014) reinterpreted the empirical relation in terms of arguments about a generalized Reynolds analogy. In this work we deploy the latest formula (Duan & Martín 2011; Zhang *et al.* 2014), which is given by

$$\frac{T}{T_e} = \frac{T_w}{T_e} + sPr\frac{U}{U_e}\frac{T_r - T_w}{T_e} + \left(\frac{U}{U_e}\right)^2 \left(\frac{T_e - T_w}{T_e} + sPr\frac{T_w - T_r}{T_e}\right), \tag{2.6}$$

where $sPr = 0.8$ (Zhang *et al.* 2014), the recovery temperature $T_r = T_e + rU_e^2/2$, and the recovery factor $r = 0.9$.

2.1. *Solving the nonlinear system for the mean profiles*

The temperature profile can be determined by solving the nonlinear system that consists of the equation of state (Eq. (2.1)), viscosity law (Eq. (2.2)), velocity law of the wall (Eq. (2.3)), velocity transformation (Eq. (2.4)), and modified Walz relation (Eq. (2.6)). This system is one-dimensional, and its solution is not resource intensive.

The nonlinear system requires several boundary conditions, which encode the non-dimensional parameters of the simulation. The compressible resolution requirements have a complex nonlinear dependence on the non-dimensional parameters of the flow. The profiles of velocity and viscosity are computed for the conditions $M_e = \{0.1, 0.5, 1.0, 2.0, 3.0\}$ and $Re_{\delta,e} = 7.5e4$. The results in Figures 1(a) and 2(a) are for $T_e/T_w = 3/2$; the results in Figures 1(b) and 2(b) are for $T_e/T_w = 1$. Note that, for a channel flow, the centerline (boundary layer edge) temperature can not be freely specified and can be iteratively determined as the condition at which $dT/dy = 0$ at the centerline.

3. Compressible grid-point requirements

The grid size of a DNS is set by the Kolmogorov scale η, which is the characteristic size of the smallest eddies in a turbulent flow. The Kolmogorov scale is defined as

$$(\eta^+)^4 = \left(\frac{\mu^+}{\rho^+}\right)^3 \frac{\rho^+}{\phi^+}, \tag{3.1}$$

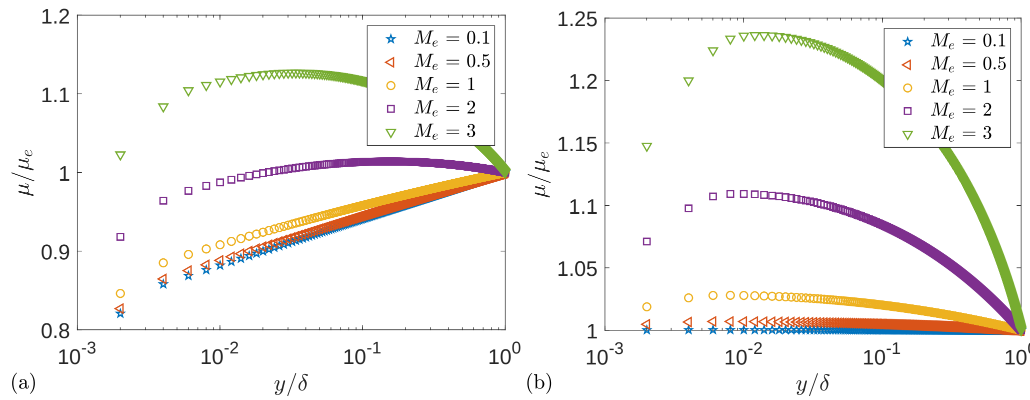

FIGURE 2. Viscosity profiles for boundary layers with $M_e = \{0.1, 0.5, 1.0, 2.0, 3.0\}$ and $Re_{\delta,e} = 7.5e4$. (a) $T_e/T_w = 3/2$. (b) $T_e/T_w = 1$.

where ϕ is the rate of dissipation of turbulent kinetic energy. The wall-normal profiles for the density and viscosity were discussed in the previous section; the dissipation rate will be discussed next.

Huang *et al.* (1995) proposed that turbulence intensities should be normalized by the local density, local viscosity, and wall shear stress. This is referred to as the semi-local non-dimensionalization and is denoted with a superscript *. It implies a semi-local velocity scale $u_{sl} = \sqrt{\tau_w/\rho}$ and a semi-local length scale $\ell_{sl} = \mu/\rho/u_{sl}$. Coleman *et al.* (1995) showed that turbulence statistics could be plotted versus $y^* = y/\ell_{sl}$ to collapse data across various Mach numbers. Zhang *et al.* (2018) simulated various various cold-wall, ideal-gas, hypersonic boundary layers. They found that profiles of the semi-local dissipation rate $\phi^* = \phi/(\rho u_{sl}^3)\ell_{sl}$ from simulations with different Mach numbers, Reynolds numbers, and wall-temperature ratios collapse when plotted against y^*. This implies that $\phi^*[y^*]$ is a Mach-invariant function, suggesting that the semi-local non-dimensionalization of the dissipation rate profile $\phi^*[y^*]$ can be modeled with incompressible channel DNS data. Specifically, the data from Lee & Moser (2015) are used.

The profile for the Kolmogorov length scale is then obtained using this dissipation rate profile and the density and viscosity profiles from the previous section. The resulting η profiles are shown in Figure 3.

The number of grid points required for accurate simulation of a DNS is found by integrating the Kolmogorov length scale over the streamwise domain $[0, L_x]$, the domain height $[0, \delta]$, and the spanwise extent $[0, L_z]$.

$$N = \int_0^{L_z}\int_0^{\delta}\int_0^{L_x} \frac{1}{\Delta_x\Delta_y\Delta_z} dxdydz = \int_0^{L_z}\int_0^{\delta}\int_0^{L_x} \frac{C_xC_yC_z}{\eta^3} dxdydz, \tag{3.2}$$

where Δ_i are the grid spacings and N_i are the number of grid points used to resolve the local Kolmogorov scale. Note that even in a channel flow, this estimate assumes that the mesh is hierarchical or unstructured so that the resolution can coarsen three dimensionally as the η grows as y increases (Yang & Griffin 2021).

If the mesh is restricted to be Cartesian and to stretch only in the y dimension, the following estimate applies

$$N_{cart} = \int_0^{L_z}\int_0^{\delta}\int_0^{L_x} \frac{C_xC_yC_z}{\eta\eta_w^2} dxdydz. \tag{3.3}$$

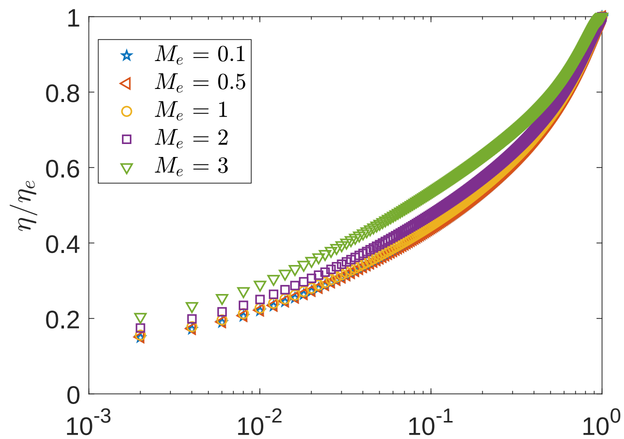

(a)

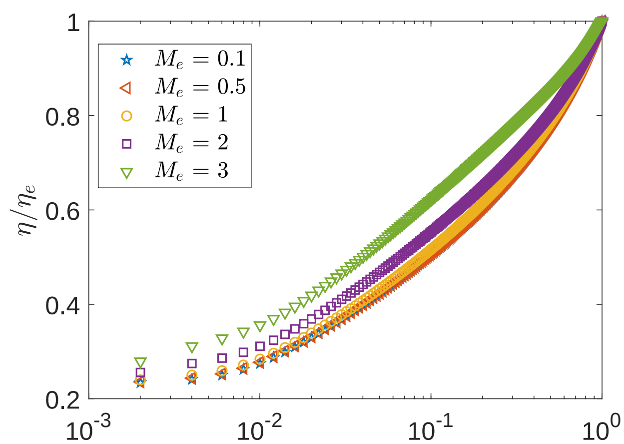

(b)

FIGURE 3. Profiles of the Kolmogorov length scale for boundary layers with $M_e = \{0.1, 0.5, 1.0, 2.0, 3.0\}$ and $Re_{\delta,e} = 7.5e4$. (a) $T_e/T_w = 3/2$. (b) $T_e/T_w = 1$.

If the additional computational cost of using a hierarchical or unstructured solver instead of a Cartesian solver does not scale with Reynolds number, then for asymptotically high Reynolds numbers the former will be less expensive. Thus, all calculations in this work assume a hierarchical or unstructured solver.

Following Choi & Moin (2012), we let $C_x C_y C_z = 125$. For a channel flow with the domain $2\pi\delta \times 2\delta \times \pi\delta$, integrating Eq. (3.2) leads to grid-point estimates for various choices of friction Reynolds number Re_τ and centerline Mach number M_c, as reported in Figure 4.

4. Compressible time-step requirements

Turbulent flows are inherently unsteady. DNS is a time-accurate simulation paradigm whose accuracy relies on temporal resolution of the relevant physical timescales. For

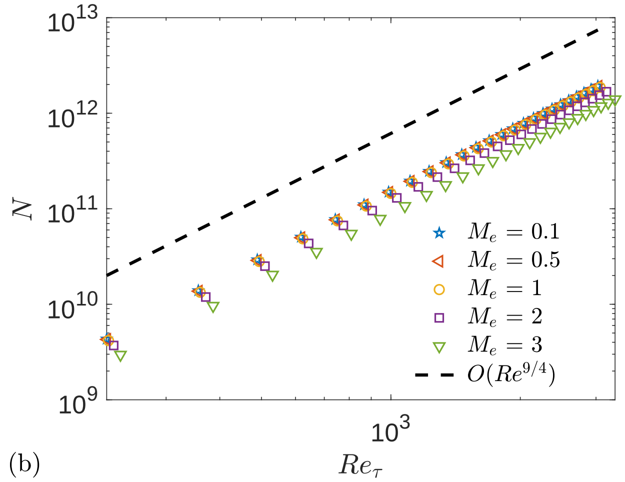

(b)

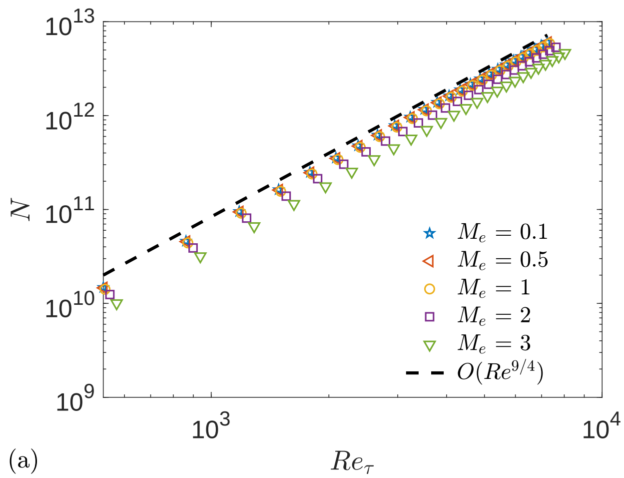

(a)

FIGURE 4. Grid-point requirements for $M_e = \{0.1, 0.5, 1.0, 2.0, 3.0\}$ and $Re_{\delta,e} = [4e3, 7.5e4]$. (a) $T_e/T_w = 3/2$. (b) $T_e/T_w = 1$.

single-phase compressible turbulence, these are the convective, acoustic, and viscous timescales. The time step thus must scale with

$$\Delta_t \leq C_c \min_i \left[\frac{\Delta_i}{U_i}\right], \tag{4.1}$$

$$\Delta_t \leq C_a \frac{\min_i [\Delta_i]}{a}, \tag{4.2}$$

$$\Delta_t \leq C_v \frac{(\min_i [\Delta_i])^2 \rho}{\mu}, \tag{4.3}$$

where C_c, C_a, and C_v are order-one constants that describe the number of time steps required to resolve the convective, acoustic, and viscous timescales, which depend on

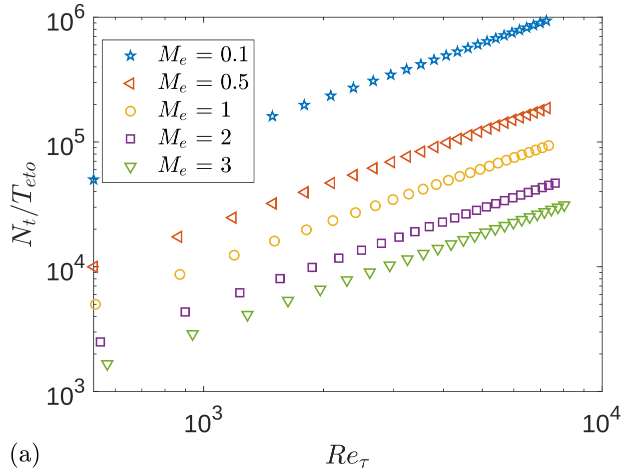

(a)

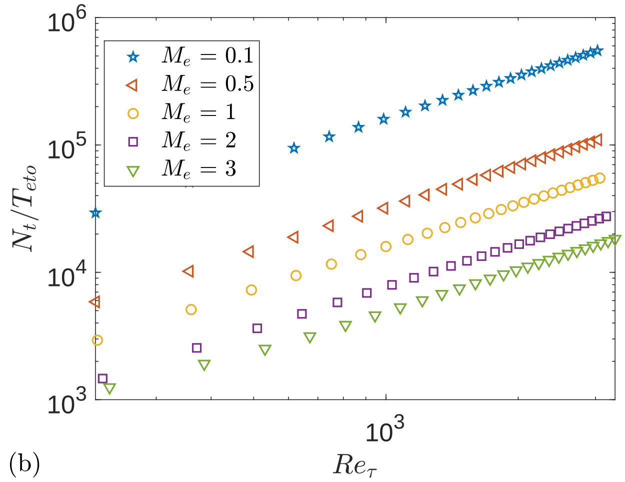

(b)

FIGURE 5. Time-step requirements for $M_e = \{0.1, 0.5, 1.0, 2.0, 3.0\}$ and $Re_{\delta,e} = [4e3, 7.5e4]$. The temperature ratio is (a) $T_e/T_w = 3/2$ and (b) $T_e/T_w = 1$.

the order of the temporal discretization and its stability properties. These numbers are sometimes referred to as the Courant-Friedrichs-Lewy (CFL), acoustic CFL, and diffusive CFL numbers. They are taken to be unity in this work. In wall-bounded flows, it is typical that the resolution is finest in the wall-normal direction and the mean flow is strongest in the wall parallel direction. This implies

$$\Delta_t \leq C_c \frac{\Delta_x}{U}, \tag{4.4}$$

$$\Delta_t \leq C_a \frac{\Delta_y}{a}, \tag{4.5}$$

$$\Delta_t \leq C_v \frac{(\Delta_y)^2 \rho}{\mu}, \tag{4.6}$$

The most restrictive of these inequalities determines the maximum allowable time step Δ_t. For a statistically stationary flow, such as a channel flow, the turbulent simulation must include a time domain that is sufficiently large to adequately sample the longest flow timescale, the eddy turnover time $T_{et} = \delta/U$. This implies that the number of time steps N_t in a simulation scales with T_{et}/Δ_t. The resulting time step is shown in Figure 5.

5. Conclusions

In compressible flows, the grid-point and time-step requirements depend on the solution due to the coupling of the velocity and temperature. This motivated reduced-order modeling of the solution, which combined several existing ingredients into an iterative method that requires only incompressible reference data and the non-dimensional parameters of the targeted compressible flow. The resulting grid-point estimates were only mildly sensitive to the Mach number (factor of 2) because the ratio of the temperature of the wall and that of the centerline was held constant. Often, this is also a function of Mach number. Generally, as the wall becomes hotter (with respect to the freestream), more grid points are required. The dependence of grid points on Reynolds number was approximately the same as in the incompressible case. The maximum allowable time step to resolve the convective, acoustic, and viscous processes was found to increase with Mach number if the ratio of the wall and freestream temperatures is held constant. Meanwhile, the maximum allowable time step decreases when the wall temperature is reduced.

Acknowledgments

K.P.G. acknowledges support from NDSEG and Stanford Graduate Fellowships. P.M. acknowledges support from NASA's Transformational Tools and Technologies project under grant number NNX15AU93A, and by Boeing Research & Technology. We wish to acknowledge helpful feedback from Mr. Christopher Williams, Dr. Sanjeeb T. Bose, and Dr. Javier Urzay.

REFERENCES

Busemann, A. 1931 *Handbuch der Experimentalphysik*, Vol. 4. Geest und Portig.

Chapman, D. R. 1979 Computational aerodynamics development and outlook. *AIAA J.* **17**, 1293–1313.

Choi, H. & Moin, P. 2012 Grid-point requirements for large eddy simulation: Chapman's estimates revisited. *Phys. Fluids* **24**, 011702.

Coleman, G. N., Kim, J. & Moser, R. D. 1995 A numerical study of turbulent supersonic isothermal-wall channel flow. *J. Fluid Mech.* **305**, 159–183.

Crocco, L. 1932 Sulla trasmissione del calore da una lamina piana a un fluido scorrente ad alta velocita. *Aerotecnica* **12**, 181–197.

Duan, L. & Martín, M. P. 2011 Direct numerical simulation of hypersonic turbulent boundary layers. Part 4. Effect of high enthalpy. *J. Fluid Mech.* **684**, 25–59.

Griffin, K., Fu, L. & Moin, P. 2021*a* Improved equilibrium wall stress model for turbulent boundary layers with zero pressure gradient. In *Proc. 25th Int. Congr. Theor. Appl. Mech.*, pp. 459–460. Milan, Italy.

Griffin, K. P., Fu, L. & Moin, P. 2021*b* Velocity transformation for compressible wall-bounded turbulent flows with and without heat transfer. *Natl. Acad. Sci. USA* **118**, e2111144118.

Guo, J., Yang, X. & Ihme, M. 2019 Thermal structures and heat transfer in wall-bounded flows at transcritical conditions. *Annual Research Briefs*, Center for Turbulence Research, Stanford University, pp. 273–284.

Huang, P. G., Coleman, G. N. & Bradshaw, P. 1995 Compressible turbulent channel flows: DNS results and modelling. *J. Fluid Mech.* **305**, 185–218.

Lee, M. & Moser, R. D. 2015 Direct numerical simulation of turbulent channel flow up to $Re_\tau = 5200$. *J. Fluid Mech.* **774**, 395–415.

Patel, A., Boersma, B. J. & Pecnik, R. 2016 The influence of near-wall density and viscosity gradients on turbulence in channel flows. *J. Fluid Mech.* **809**, 793–820.

Trettel, A. & Larsson, J. 2016 Mean velocity scaling for compressible wall turbulence with heat transfer. *Phys. Fluids* **28**, 026102.

Walz, A. 1969 *Boundary Layers of Flow and Temperature*. MIT press.

Yang, X. I. A. & Griffin, K. P. 2021 Grid-point and time-step requirements for direct numerical simulation and large-eddy simulation. *Phys. Fluids* **33**, 015108.

Zhang, C., Duan, L. & Choudhari, M. M. 2018 Direct numerical simulation database for supersonic and hypersonic turbulent boundary layers. *AIAA J.* **56**, 4297–4311.

Zhang, Y. S., Bi, W. T., Hussain, F., Li, X. L. & She, Z. S. 2012 Mach-number-invariant mean-velocity profile of compressible turbulent boundary layers. *Phys. Rev. Lett.* **109**, 054502.

Zhang, Y. S., Bi, W. T., Hussain, F. & She, Z.-S. 2014 A generalized Reynolds analogy for compressible wall-bounded turbulent flows. *J. Fluid Mech.* **739**, 392–420.